International Journal of Thin Films Science and Technology

http://dx.doi.org/10.12785/ijtfst/040110

Nano Wall Growth and Structural, Electro-Optical Characterization of Spray Pyrolytic Cobalt Oxide Thin Films.

M. M. Islam[1], *M. G. M. Choudhury*[2], *M. M. Rahman*[3], *M. K. R. Khan*[3,*], *M. Shahjahan*[4] *and K. Uddin*[5].

[1]Bangladesh Atomic Energy Regulatory Authority, Dhaka-1207. Bangladesh.
[2]Department of Electronics and Telecommunication Engineering, Daffodil International University, Bangladesh.
[3]Department of Physics, Rajshahi University, Rajshahi- 6205, Bangladesh.
[4]Department of Applied Physics, Bangabandhu Sheikh Mujibur Rahman Science and Technology University, Gopalganj-8100, Bangladesh.
[5]Department of Physics, Jagannath University, Dhaka-1100, Bangladesh.

Received: 2 Aug. 2014, Revised: 14 Nov. 2014, Accepted: 18 Nov. 2014.
Published online: 1 Jan. 2015.

Abstract: Cobalt oxide thin films were deposited by spray pyrolysis method onto a glass substrate at 300°C substrate temperature. Structural, optical and electrical properties of the films were studied. The crystal structure of as-deposited and annealed samples was determined by X-ray diffraction (XRD) analysis. The structure of cobalt oxide was found to be cubic with lattice constant is $a \sim 0.4$ nm. The spectral absorption coefficient (α) at the fundamental absorption region was determined using the spectral data of transmittance and reflectance. The band gap energies were determined depending on the film thickness and the values obtained were vary from 1.357 eV to 1.440 eV for CoO phase and 1.474 eV to 1.516 eV for Co_3O_4 phase, respectively depending on film thickness. The refractive index and dielectric constant were calculated from reflectance and transmittance data. Refractive index varies from 1 to 2.8. From the thermal emf measurements the thermoelectric power S, the scattering factor A, low temperature activation energy E_0 and coefficient of activation energy γ have also been calculated. The values of A lies between 1.1 to 1.28 suggesting that the scattering is due to lattice vibration and the position of Fermi energy at low temperature, E_0 (~ 0.0002 eV) suggests that Fermi level is just on the top edge of valance band. At room temperature activation energy becomes ~ 0.29 eV, which indicates that the Fermi level is inside the forbidden energy gap.

Keywords: Nanowall growth, XRD, Spray Pyrolysis, Thermoelectric power.

1.Introduction

The development of contemporary sophisticated technologies which increase the quality of human life is closely related to the semiconducting materials. The science and technology of semiconducting thin films have a crucial role in high-tech industry. Thin film of semiconducting materials is applicable in the field of microelectronic, optoelectronic, communication technologies, as well as in energy generation and conservation strategies, etc. [1].

Cobalt oxide is one of the versatile oxide materials among the transition metal oxides. It is a p-type anti-ferromagnetic oxide semiconductor with a Neel temperature, T_N, of 290 K. Cobalt oxide (both CoO and Co_3O_4 phases) has emerged as a good candidate for high-temperature solar selective absorbers [2-7] and is used as a catalyst in the hydro-cracking process of crude fuels, as a pigment for glasses and ceramics, and as an electro-chromic material [8]. It has direct band gap of 2.06-1.44 eV, and indirect band gap of 1.38-1.26 eV [9].Considering its importance a variety of techniques have been applied to deposit cobalt oxide thin films, such as anodic electro-precipitation [8], electro-deposition [3], oxidation of an electroplated thin cobalt layer [4], the dip coating process [5], pulsed liquid injection chemical vapor deposition [10], sol-gel [11] and the spray pyrolysis technique [7,9]. In the method of spray pyrolysis reported earlier [7, 9] cobalt oxide films were deposited on stainless steel and glass substrate. This paper presents the surface morphology, optical, electrical and thermal properties of pyrolized nano morphological films of cobalt oxide deposited onto glass substrate.

2. Experimental section

2.1. Films preparation

Cobalt oxide thin films were deposited by spraying the aqueous solution of 0.1M of $[Co(CH_3COO)_2].4H_2O$ onto preheated glass substrate. The substrate temperature was maintained at 300 ºC. Spray pyrolysis is basically a

*Corresponding author e-mail: fkrkhan@yahoo.co.uk

chemical process that involved in spraying of the solution. The spray solution was sprayed from ~25 cm apart onto a substrate held high temperature where the solution reacts forming the desired film. The flow rate of the solution during spraying was adjusted to about 2.5 ml-min^{-1} and kept constant throughout the experiment. The temperature of the substrate was controlled by a copper-constantan thermocouple.The possible chemical reaction that takes place on the heated substrate to produce cobalt oxide is given as follows:

$$Co(COOCH_3)_2 .4H_2O \xrightarrow{\text{Decomposed at 300 ºC}} (Co_3O_4+CoO)$$
$$+CO_2\,(g)+CH_4\,(g)+\text{steam}\,(g)$$

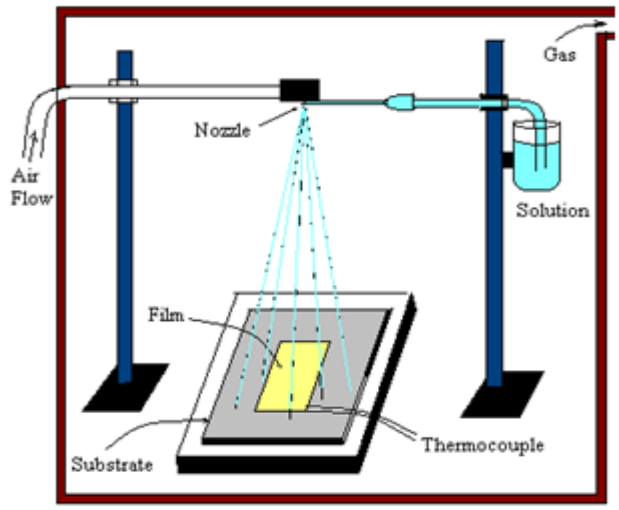

Fig.1: Setup for spray Pyrolysis unit

2.2. Film characterization

The thickness of cobalt oxide films was measured by Fizeau-fringes method. The structural properties were studied by X-ray diffraction measurements using PW 3040 X'Pert PRO XRD System. Cu K_α radiation was used whose primary beam power was 40 kV and 30 mA. All the samples were scanned over 2θ range from 10° to 70° to get possible fundamental peaks of the sample with the sampling step of 0.02° and time for each step data collection was 1.0 sec. All data of samples were analyzed by using computer software "X'PERT HIGHSCORE" from which structural parameter was determined. The surface properties of the films were examined by using HITACHI S-3400N model Scanning Electron Microscope (SEM) attached with an EDX to measure quantitatively the sample stoichiometry. Optical transmittance and reflectance spectra with respect to glass substrate measurements were carried out within the wavelength range 600 nm to 1100 nm using UV-1601 PC SHIMADZU scanning double beam spectrophotometer (not shown). The experimental accuracy of the transmittance and reflectance is (±0.005%) and wavelength is (±0.005%).

Van der Pauw's method was used for resistivity measurements using Keithley electrometer. The temperature dependence electrical resistivity, ρ was measured within the temperature range 300 K to 450 K. The Copper-Tungsten thermocouple was used to determine the temperature and indium was used for Ohmic contacts.

3. Results and Discussion

3.1 Structural Properties

X-ray diffraction patterns obtained for cobalt oxide is shown in Fig.2. XRD patterns of as-deposited film (Fig.2a) show a broad peak around 2θ = 23° and having a small peak near 2θ = 37°. This result indicates that as-deposited films are mainly amorphous and also contains some small crystallites. On annealing the film at 350 °C in air for one hour, a number of highly resolved characteristic peaks have been developed (Fig.2b), but the broad peak with less intensity remains in the XRD patterns. The existence of broad peaks after annealing indicates that amorphous phase is still left in the film but material is mostly polycrystalline. The characteristic peaks for crystalline structure were identified comparing with standard JCPDS card and these are at 2θ = 18.84°, 31.22°, 36.42°, 59.1°, 65.5° having (h k l) value (111), (220), (100), (511), (440), respectively for Co_3O_4 phase and for CoO phase peak position was at 2θ = 44.36° having (h k l) value (400). The crystal structure for both phases has been identified as cubic. Lattice constant has been calculated using the dominant peaks for Co_3O_4 and the average value obtained is, $a \cong 0.400$ nm, which is very closed to the standard value $a = 0.422$ nm.

3.2 Surface morphology

Surface morphology of cobalt oxide samples having thickness of ≈150 nm was studied by scanning electron microscopy under X500, X2000 and X5000 magnifications. The surface of the film was found to be smooth, uniformly covered the whole surface of the substrate. The SEM image under X500 magnifications shows some spherical structures bounded by many rings of almost equal diameter as Fig.3a (i) and inside the sphere there are large numbers of nano-walls exist as shown in Fig.3a (ii). Under higher magnification X5000, it is clear that these nano-walls are randomly distributed on the film surface as is shown in Fig.3a (iii).

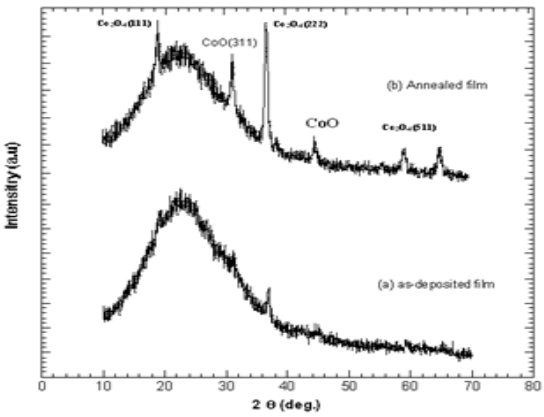

Fig.2: XRD spectra of cobalt oxide thin films deposited on glass substrate.

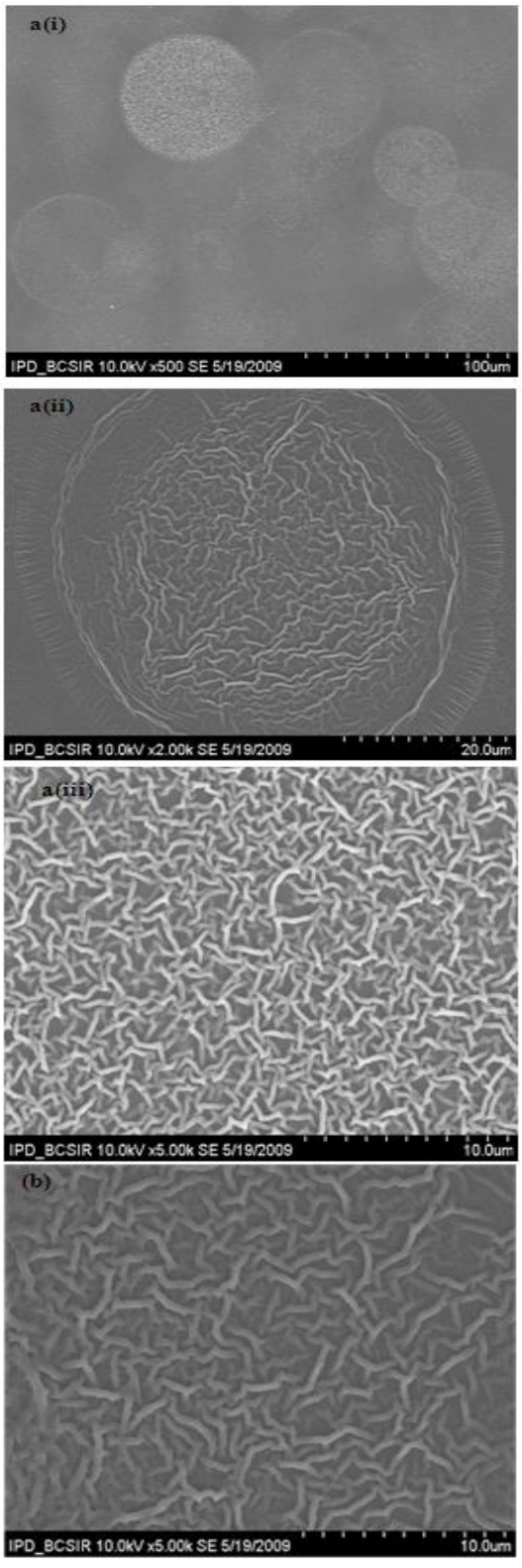

Fig.3: SEM micrographs:

(a) as-deposited films at different magnifications:
(i) X500, (ii) X2000, (iii) X5000;
(b) annealed at 350ºC for 1 hour and magnification X5000.

3.3 Optical properties

3.3.1 Absorption coefficient

The absorption coefficient (α) data were calculated from transmittance (T) and reflectance (R) data of cobalt oxide thin films of different thickness deposited on glass substrate at substrate temperature 300 ºC. The calculation was done using the relation,

$$\alpha = \frac{1}{t}\ln\left[\frac{(1-R)^2}{T}\right] \quad (1)$$

Where t is the thickness of the film. Fig. 4 shows the variation of α with photon energy and it can be seen that the absorption coefficient first increases slowly in the low energy region i.e., in the high wavelength region and then increases sharply near the absorption edge. Finally, α value tends to become saturated at higher energy (≥1.6 eV). The absorption coefficient also increases as the film thickness increases. For higher photon energy the value of absorption coefficient is $>10^4 cm^{-1}$.

The direct band gap energy of the films has been obtained from the intercept on the energy axis after extrapolation of the straight line section of Fig.5. The indirect band gap energy is obtained in similar fashion as we did for direct transition as shown in Fig.6. Optical band gap obtained for direct and indirect transitions are given in Table-1.

Table 1: Optical band gaps for direct and indirect transitions

Film thickness, t in nm	Direct band gap Energy, E_g in eV	Indirect band gap Energy, E_g in eV
105	1.516	1.440
150	1.509	1.421
195	1.501	1.402
225	1.491	1.381
320	1.474	1.357

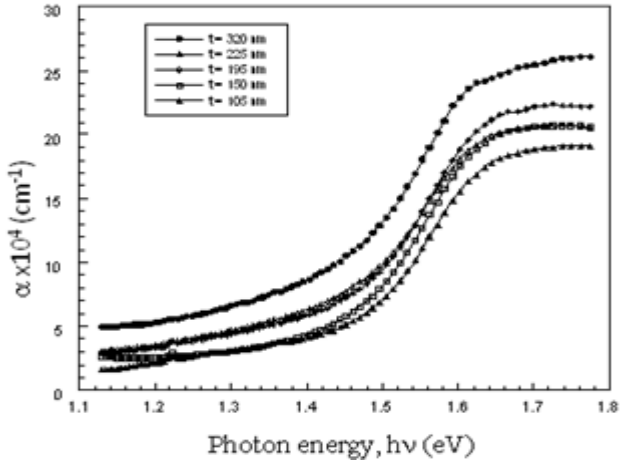

Fig. 4 Variation of absorption coefficient as a function of photon energy for cobalt oxide films of different thickness.

3.3.2 Refractive index and extinction coefficient

The refractive index, n_r, and extinction coefficient, k, are determined by computing the reflection and transmission data using the relations,

$$R = \frac{(1-n_r)^2 + k^2}{(1+n_r)^2 + k^2} \quad (2)$$

$$k = \frac{1}{4\pi t}\ln\left[\frac{(1-R)^2}{T}\right] \quad (3)$$

Where, t is the film thickness.

The variation of refractive index, n_r, and extinction coefficient, k, with photon energy for cobalt oxide thin films of different thicknesses are shown in Figs. 7 and 8, respectively.

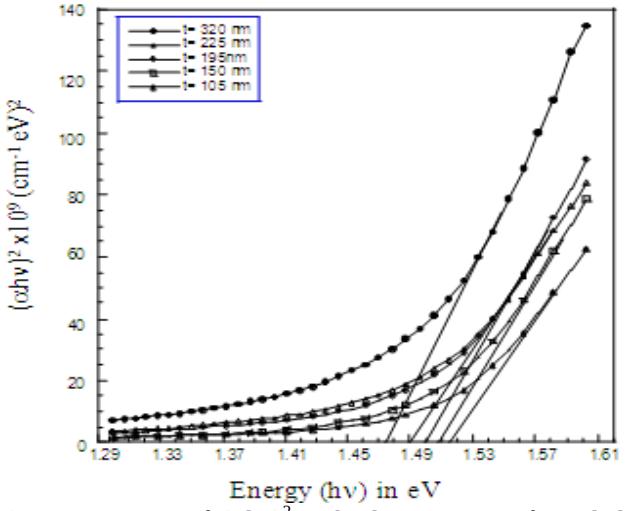

Fig. 5: Variation of $(\alpha h\nu)^2$ with photon energy for cobalt oxide films of different thickness.

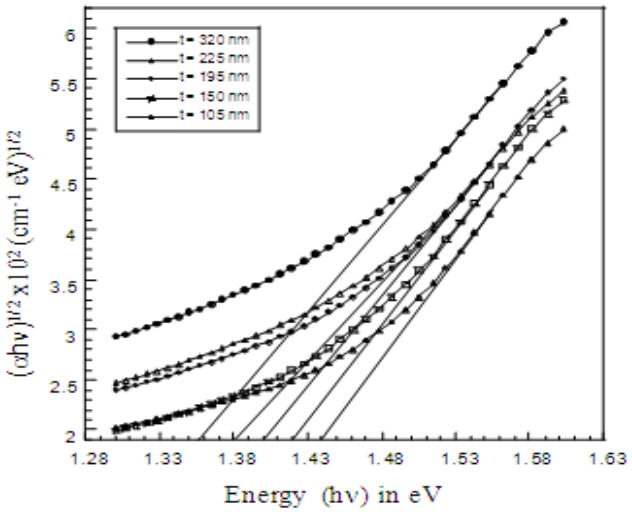

Fig.6: Variation of $(\alpha h\nu)^{1/2}$ with photon energy for cobalt oxide films of different thickness.

From figures it is observed that the refractive index gradually increases with photon energy and goes to a maximum value and then decreases as the energy increases. The refractive index of the films varies with film thickness as well. However, the extinction coefficient is gradually increases in the lower energy region and when the energy exceeds band gap energy it increases to a maximum value and then decreases. The gradual increase of refractive index with photon energy implies that the normal dispersion occurred before the absorption edge followed by an anomalous dispersion.

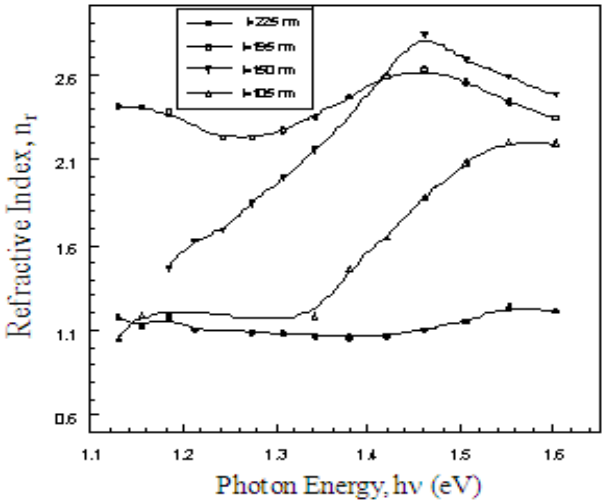

Fig.7: Variation of refractive index with photon energy for cobalt oxide thin films of different thickness.

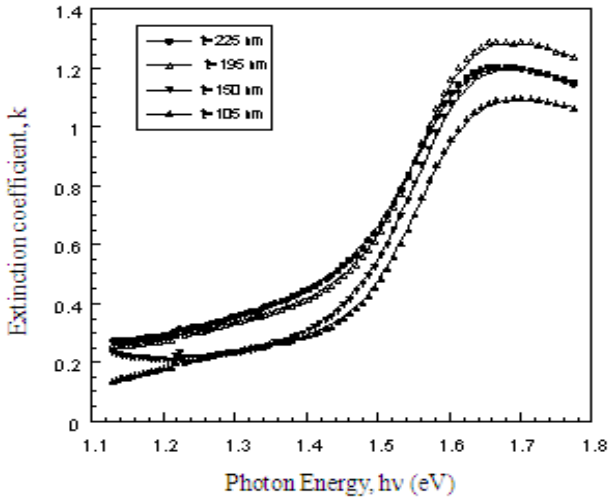

Fig.8: Variation of extinction coefficient with photon energy for cobalt oxide films of different thickness.

3.3.3 Dielectric constant

The real and imaginary part of dielectric constant of cobalt oxide films were determined by the following relations,

$$\varepsilon_r = n_r^2 - k^2 \text{ and } \varepsilon_i = 2n_r k \quad (2)$$

The variation of the real (ε_r) and imaginary (ε_i) parts of dielectric constant for different thicknesses are shown in Fig.9 and 10, respectively. Figures show that ε_1 and ε_2 varies with photon energy as well as with thickness of the film. The value of real part of dielectric constant is slightly higher than the imaginary part of dielectric constant.

3.4 Electrical properties

3.4.1 Resistivity measurement

Resistivity measurements are made for a few freshly deposited films from room temperature to 450 K by van der Pauw method.

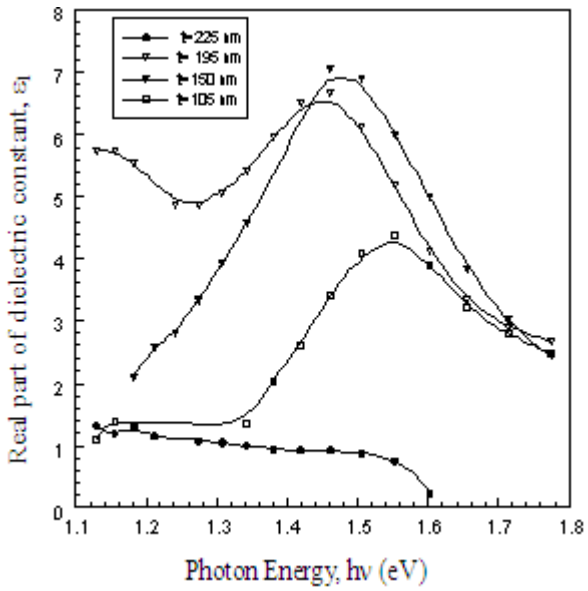

Fig.9: Variation of real part of dielectric constant with photon energy for cobalt oxide films of different thickness.

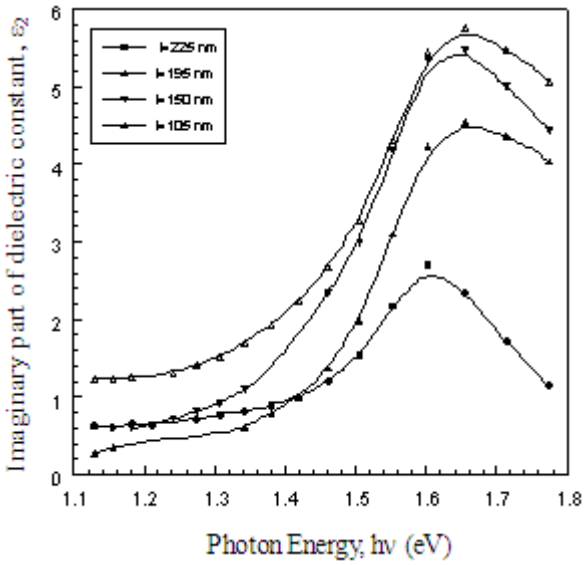

Fig.10: Variation of imaginary part of dielectric constant with photon energy for cobalt oxide films of different thickness.

At maximum temperature (450 K), films are annealed for one hour and then cool down slowly to room temperature (RT). The resistivity of the sample was measured again with increasing temperature. Variation of resistivity with temperature for one film during heating, cooling and reheating is shown in Fig.11. It is seen that resistivity shows a non-reversible behavior between first heating and cooling cycles. However, resistivity under one hour annealed sample shows reversibility on repeated cycle of heating and cooling and eventually retraces the same paths indicating a stable state of the film. The stability of the film is seems to be due to the removal of meta-stable phases, in homogeneity, strain and defects that usually present in the virgin samples.

Table 2: Activation energies ΔE_1 and ΔE_2

Film thickness, t in nm	Activation energy ΔE_1 in eV	Activation energy ΔE_2 in eV
200	0.219	0.432
250	0.217	0.424
300	0.212	0.308

The variation of logarithmic conductivity with inverse temperature is shown in Fig.12. It is revealed that the conductivity increases monotonically with increasing temperature up to 450 K as well as film thickness.

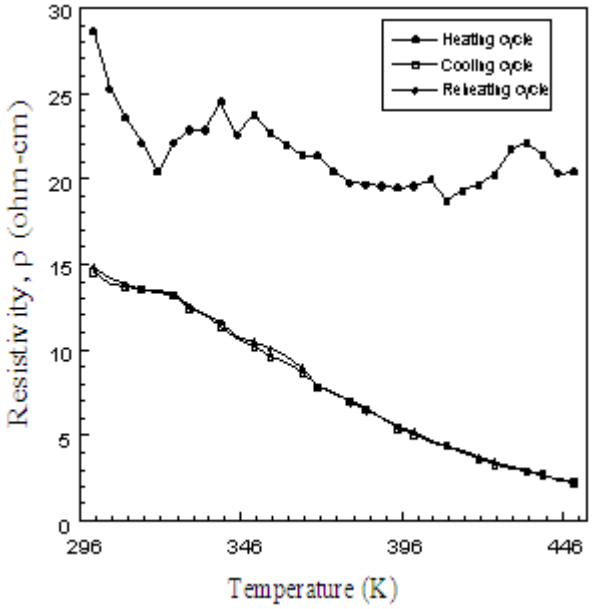

Fig.11: Variation of resistivity with temperature for cobalt oxide film.

The d.c electrical conductivity of the thin films can be expressed by the usual relation,

$$\sigma_f = \sigma_0 \exp\left(-\frac{\Delta E}{2k_b T}\right) \quad (5)$$

Where ΔE is the activation energy, k_b is the Boltzmann constant and σ_0 is the pre-exponential factor. Following this relation the activation energy for low temperature region, ΔE_1, and for high temperature region, ΔE_2, was calculated from the slope of the plot 12. The values obtained are given in Table 2.

The activation energy ΔE_2 is higher than that of ΔE_1. Since the films are well conducting, the obtained activation energies indicate that the transition occurred from localized state to valance band.

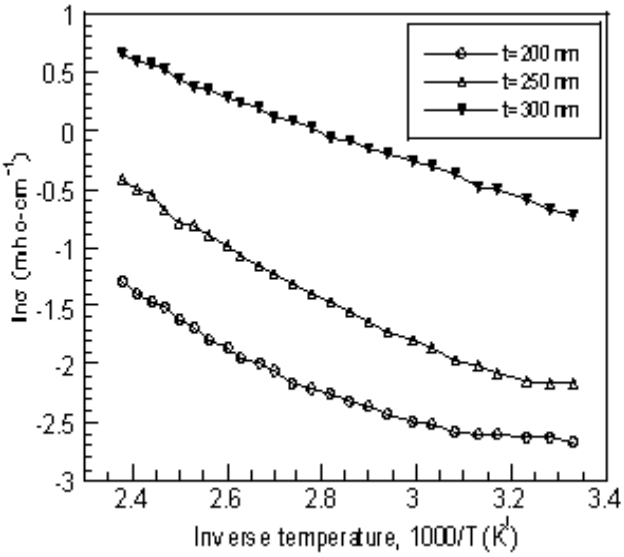

Fig.12: Variation of logarithmic conductivity with inverse temperature.

3.4.2 Thermoelectric power measurement

The thermal emf of cobalt oxide thin films of a different set of film thicknesses have been measured in the temperature range 300-460 K using a digital meter keeping positive terminal of the meter to the hot junction of the sample and negative terminal to the cold junction. The emf generated between hot and cold junction was negative at room temperature and this negative value increases with the increase of temperature. This negative emf at room temperature revealed that the samples are of p-type materials.

The thermoelectric power, S of the samples was calculated from the thermal emf by using the relation,

$$S = \pm \Delta V / \Delta T \quad (6)$$

The variation of the thermoelectric power, S with inverse of temperature is shown in Fig. 13. The thermoelectric power for p-type semiconductor can be represented by the relation,

$$S=\frac{k}{e}\left(\frac{E_F-E_V}{k_bT}+A\right) \quad (7)$$

where, E_F is the position of the Fermi energy, E_V is the top of the valence band energy and A is scattering factor which varies from 0 to 4 depending on the nature of scattering process involved in transport mechanism. The scattering factor A is determined by the intercept on y-axis at $1/T\approx 0$. For the limited range of temperature we may write

$$E_F-E_V=E_0-\gamma T \quad (8)$$

And then S can be written as:

$$S=\frac{k}{e}\left(\frac{E_0}{kT}-\frac{\gamma}{k}+A\right) \quad (9)$$

The Peltier coefficient, $\prod$ is given as:

$$ST=\prod=\frac{k}{e}\left[\frac{E_0}{k}-\left(\frac{\gamma}{k}-A\right)T\right] \quad (10)$$

Where γ is the coefficient of low temperature activation energy and Π is the Peltier coefficient. Fig. 14 shows the variation of Peltier coefficient, Π with temperature. The value of E_0 has been calculated from the intercept on y-axis at $T\approx 0$, where the values of γ were determined from the slope of Π vs. T curve. The values of scattering factor A for all the samples are almost equal to 1, implied that the scattering involved for all samples may be due to lattice scattering. The value of A, γ and E_0 are given in Table 3. The scattering index r can be obtained from parameter, $A=r+5/2$. The values of r obtained in this study are negative and less than -3/2 ($r<-3/2$). If one correlate scattering index classically to the T^r dependence of mobility μ, then the value of $r=-3/2$ is for phonon scattering. The obtained values of r in this study imply that hole-phonon scattering process is involved in the carrier transport process of the films.

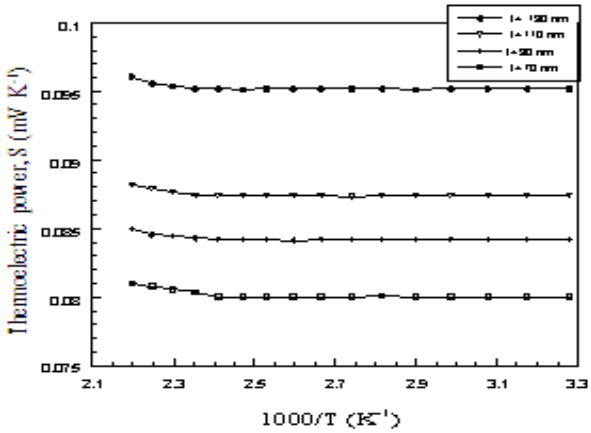

Fig.13: Variation of thermoelectric power with inverse temperature for cobalt oxide films of different thickness.

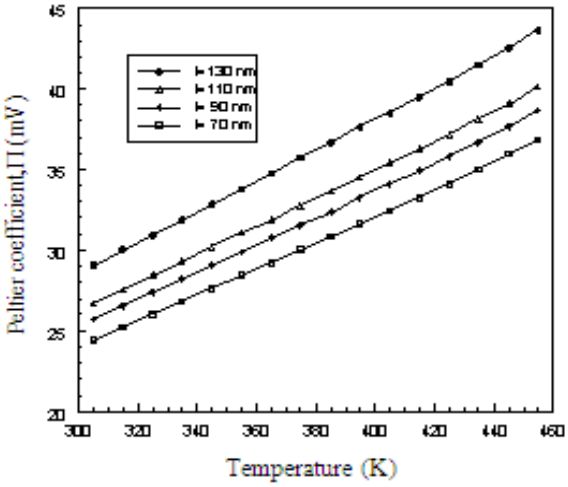

Fig.14: Variation of peltier coefficient with temperature for cobalt oxide films of different thickness.

The value of E_0 (position of Fermi energy at low temperature) is very low, i.e., E_F is just on the edge of valance band energy and it goes out to the forbidden band energy at room temperature. The value of scattering factor A for all the samples are nearly equal to 1, from which it can be said that the scattering involved for all the sample may be due to lattice scattering.

Table 3. Data for A, γ and E_0

Thickness (nm)	Scattering factor, A	γ x10^{-4} (eV/K)	E_0x10^{-4} (eV)
130	1.28	10.7	2.0
110	1.17	9.8	
90	1.12	9.5	
70	1.1	9.00	

4. Conclusion

Cobalt oxide nano-wall thin films of different thicknesses have been prepared by inexpensive spray pyrolytic technique onto glass substrate at 300 °C. The SEM

micrograph shows that films are well adherent, homogeneous, and smooth and nano fiber structures appear around the nucleation center. The films are highly conducting and transparent with small reflectivity in the visible spectra range, may be suitable for window layer applications. The nature of thermo-power and optical band gap energy suggest that cobalt oxide is a p-type semiconductor.

Acknowledgement

The first author acknowledges Rajshahi University for providing partial experimental assistance.

References

[1] Pejova Biljana, Atanas Tanusevski, and Ivan Grozdanov, *Journal of Solid State Chemistry* **172**, p381-388, (2003).

[2] J. G. Cook and F. P. Koffyberg, *Solar Energy Mater* **10**, 55, (1984).

[3] G. E. McDonald, *Thin Solid Films* **72**, 83, (1980).

[4] G. B. Smith, A. Ignatiev and G. Zajac, *J. Appl. Phys.* **51**, 4186, (1980).

[5] K. J. Cathro, *Solar Energy Mater* **9**, 433, (1984).

[6] C. M. Lampert, *Thin Solid Films* **72**, 73, (1980).

[7] K. Chidambaram, L. K. Malhotra and K. L. Chopra, *Thin Solid Films* **87**, 365, (1982).

[8] T. Seike and J. Nagai, *Solar Energy Mater* **22**, 107, (1991).

[9] P. S. Patil, L. D. Kadam, C. D. Lokhande, *Thin Solid Films* **272**, 29, (1996).

[10] D. Mehandjiev and E. Nikolova-Zhecheva, *Thermochim. Acta* **32**, 145, (1980).

[11] R. H. Misho and W. A. Murad, *Solar Energy Mater Solar Cells* **2,** 335, (1992).

[12] L. M. Apatiga, V. M. Castano, *Thin Solid Films* **496,** 576, (2006).

[13] V. Musat, E. Fortunato, A. M. Botelho do Rego, R. Monteiro, *Thin Solid Films* **516**, 1499, (2008).

[14] M. R. Islam and J. Podder, *Cryst. Res. Technol.* **44,** 286, (2009).